2
Modeling and Classical Control Design

In this chapter, the problem of the modeling and classical control design of the Tracked Mobile Robot is aimed. Using a kinematic model and considering the slipping factor, two new theorems are introduced in order to control the TMR using the Cartesian approach and Polar coordinates approach. Additionally, some numerical simulations are presented in order to validate the proposed controllers.

2.1
Description of a Tracked Mobile Robot

The main feature and advantage of the Tracked Mobile Robot is the large contact area with the soil, giving it high mobility in unstructured environments, although it comes with a complex kinematic model compared to others mobile robots such as: unicycle, car-like Ackerman or skid steering. In this section, firstly we introduce the model of the robot and its features and the main parts of a TMR, next the kinematic model of the robot will be described.

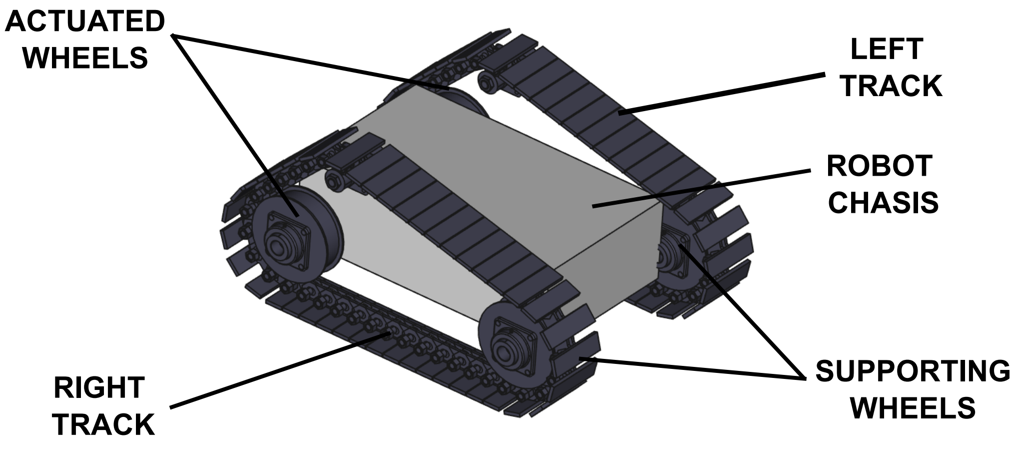

Figure 2.1: Tracked Mobile Robot.

The Tracked Mobile Robot used in this work is presented in Figure 2.1. It has two independent tracks, actuated and non actuated wheels (supported wheels). In the literature, there are other types such as of TMR: there is a one with mobile arms generally used to climb stairs, a TMR with a manipulator to perform task and a TMR with multiple tracks for applications such as pipeline inspection. The tracks are also named inner (left) and outer (right) with respect to the ICR [65].

Tracks are supported by wheels mechanism that transmits the locomotion. Generally in a simple track, one of them is actuated by a motor and the others support the locomotion as can is illustrated in Figure 2.1.

2.2 Modeling

The process of modeling is in charge of motion prediction in a mobile robot given a control input. The calculation of the kinematic model is necessary to perform on board real-time computations for autonomous navigation. This section will cover the kinematic model formulation of the Tracked Mobile Robot.

2.2.1 Kinematic Modeling

Tracked Mobile Robots have similar locomotion to the skid-steering mechanisms, increasing the probability of slippage, covering this aspect the kinematic model formulation can be done using some ideas of the skid steering and considering the slippage as a time-variant variable [63]. Two assumptions are necessary (i) the robot performs locally planar motions, (ii) angular velocity of the robot is relatively small.

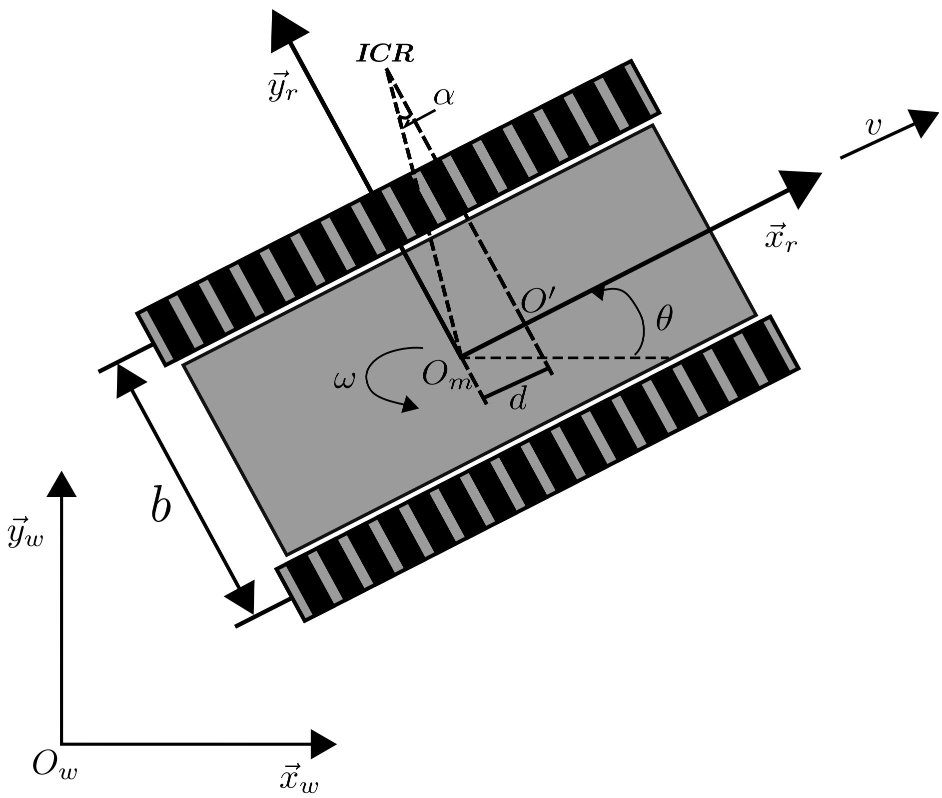

Figure 2.2: Tracked Mobile Robot Kinematic Model.

In Figure 2.2, the scheme for the Kinematic Model formulation is shown: Let us define the following coordinates systems: $\mathcal{F}_r = [\vec{x}_r \ \ \vec{y}_r]$ denotes the robot frame with origin in the center of mass of the robot (O_m), $\mathcal{F}_w = [\vec{x}_w \ \ \vec{y}_w]$ the world frame (or the inertial frame). Additionally, any configuration of position and orientation for the robot can be expressed as $q = [\, x \ y \ \theta \,]^\mathsf{T}$ relative to the inertial frame $\mathcal{F}_w$.

In order to transform one point or configuration in the robot frame $\mathcal{F}_r$ to the world frame $\mathcal{F}_w$, it is necessary a rotation matrix such as:

$$R_w^r = \begin{bmatrix} \cos(\theta) & -\sin(\theta) & 0 \\ \sin(\theta) & \cos(\theta) & 0 \\ 0 & 0 & 1 \end{bmatrix}, \qquad (2\text{-}1)$$

where θ is the orientation of the robot, with respect the inertial frame ($\mathcal{F}_w$) as can be seen in Figure 2.2.

The motion of the robot is guided by two components: linear and angular velocity (see Figure 2.2): The linear velocity v is composed by the two velocities on each axis of the frame $\mathcal{F}_w$ it means: $v = [\, v_x \ v_y \,]^\mathsf{T} = [\, \dot{x} \ \dot{y} \,]^\mathsf{T}$, the other component is the angular velocity $\omega = \dot{\theta}$.

According to the Figure 2.2, ICR is the Instantaneous Center of Rotation (ICR), it is worth noting that the slipping occurs in the v_y and because of this the center of mass of the robot (O_m) shifts by the distance d to a new center of mass O'. The angle α is between the line that connects the original center of mass O_m and I, and the perpendicular from I to the axis x_r of the robot's frame $\mathcal{F}_r$ (See Figure 2.2).

In robot frame $\mathcal{F}_r$ a suitable kinematic model for a TMR is:

$$\begin{bmatrix}\dot{x}_r\\ \dot{y}_r\\ \dot{\theta}_r\end{bmatrix} = \begin{bmatrix}\dfrac{r}{2} & \dfrac{r}{2}\\ \dfrac{-rd}{b} & \dfrac{rd}{b}\\ \dfrac{-r}{b} & \dfrac{r}{b}\end{bmatrix}\begin{bmatrix}\dot{\phi}_L\\ \dot{\phi}_R\end{bmatrix}, \tag{2-2}$$

where b is the distance between the two tracks; r is the radius of the actuated wheels; $\dot{\phi}_L$ and $\dot{\phi}_R$ are the angular velocities on each track.

Now, using the transformation in equation (2-2), the kinematic model of Tracked Mobile Robot in the Inertial frame $\mathcal{F}_w$ is given by:

$$\begin{bmatrix}\dot{x}\\ \dot{y}\\ \dot{\theta}\end{bmatrix} = \begin{bmatrix}\cos\theta & d\sin\theta\\ \sin\theta & -d\cos\theta\\ 0 & 1\end{bmatrix}\begin{bmatrix}v\\ \omega\end{bmatrix}, \tag{2-3}$$

where d is the slippage coefficient for the TMR, and v is the linear velocity and ω is the angular velocity.

Equation (2-3) can be rewritten as $\dot{q} = G(q)\,V$, V can be expressed in terms of the individual velocity of each track $\dot{\phi}_L$ and $\dot{\phi}_R$:

$$V = \begin{bmatrix}v\\ \omega\end{bmatrix} = \begin{bmatrix}\dfrac{r\dot{\phi}_L + r\dot{\phi}_R}{2}\\ \dfrac{-r\dot{\phi}_L + r\dot{\phi}_R}{b}\end{bmatrix}. \tag{2-4}$$

By defining $u = [\dot{\phi}_L\ \dot{\phi}_R]^{\mathsf{T}}$ as the real control input on each track, and can be used to control V based on the relationship $V = T\,u$:

$$V = r\begin{bmatrix}\dfrac{1}{2} & \dfrac{1}{2}\\ -\dfrac{1}{b} & \dfrac{1}{b}\end{bmatrix}\begin{bmatrix}\dot{\phi}_L\\ \dot{\phi}_R\end{bmatrix}. \tag{2-5}$$

The relationship $u = T^{-1}\,V$ from equation (2-5) is given by:

$$\begin{bmatrix}\omega_L\\ \omega_R\end{bmatrix} = T^{-1}\begin{bmatrix}v\\ \omega\end{bmatrix} = \frac{1}{rb^2}\begin{bmatrix}1 & -\dfrac{b}{2}\\ 1 & \dfrac{b}{2}\end{bmatrix}\begin{bmatrix}v\\ \omega\end{bmatrix}. \tag{2-6}$$

Since transformation T is always non-singular, it can be observed that equation (2-2) is the kinematic model of the Tracked Mobile Robot.

Notice that velocity of slipping $\dot{y} = -\omega\, d$ (see equations (2-2) and (2-4)), is not integrable, so the non-holonomic constraint [63] can be obtained as:

$$\begin{bmatrix} \sin\theta & -\cos\theta & d \end{bmatrix} \begin{bmatrix} \dot{x} \\ \dot{y} \\ \dot{\theta} \end{bmatrix} = A\dot{q} = 0\,. \tag{2-7}$$

In order to define the slipping coefficient we used the relationship [63]:

$$d = k\omega^2\,. \tag{2-8}$$

This equation is based on the soil parameter (k) and the angular velocity (ω) that affects the centrifugal forces.

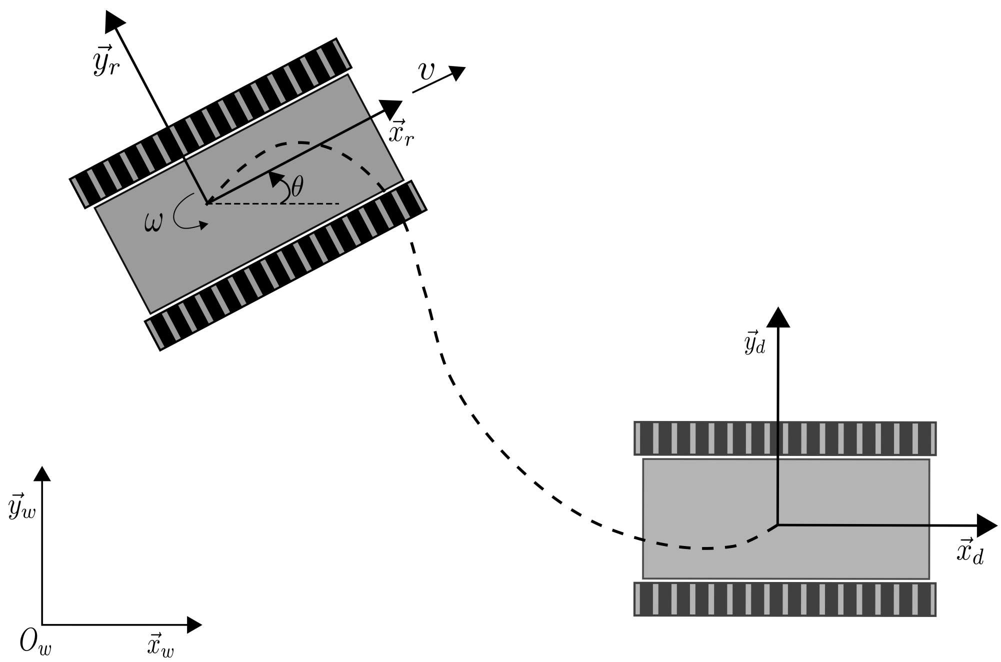

Figure 2.3: Regulation task.

2.3 Regulation Control

Regulation is the process of moving a Tracked Mobile Robot from current configuration $q = [\,x \;\; y \;\; \theta\,]^{\mathsf{T}}$ to a desired configuration $q_d = [\,x_d \;\; y_d \;\; \theta_d\,]^{\mathsf{T}}$. This task can be seen in Figure 2.3, in which the TMR is going from current frame $\mathcal{F}_r = [\,\vec{x}_r \;\; \vec{y}_r\,]^{\mathsf{T}}$ to the desired frame $\mathcal{F}_d = [\,\vec{x}_d \;\; \vec{y}_d\,]^{\mathsf{T}}$, additionally in this figure the inertial frame $\mathcal{F}_w = [\,\vec{x}_w \;\; \vec{y}_w\,]^{\mathsf{T}}$ can be observed as a reference.

2.3.1
Cartesian Coordinates based Controller

In this section, the formulation process of a new theorem in order to control the TMR in regulation task is described. This initial approach to deal with the regulation control design, is addressing the problem *partially*, where the regulation task consists of driving the TMR to a desired configuration $q_d = [\, x_d \;\; y_d \;\; \theta_d \,]^\mathsf{T}$ without considering the final orientation θ_d, this approach is called *Cartesian regulation* [2].

This approach can be useful for a number of practical tasks, such as surveillance in agricultural fields in which the TMR has to visit a sequence of well-known Cartesian positions (or *checkpoints*) repetitively in order to patrol the crop area, to perceive the characteristics of the environment using its on-board sensors. In the surveillance task, the final orientation of the TMR is not a strict requirement.

2.3.1.1
Control Design

In order to design a suitable controller to perform the regulation task, the key idea is to define the goal or the desired Cartesian configuration as $q_{d_c} = [\, x_d \;\; y_d \,]^\mathsf{T}$ as it can be seen in Figure 2.3. Now, the control strategy consists in moving the mobile robot from a initial configuration $q_c = [\, x \;\; y \,]^\mathsf{T}$ to the desired configuration q_{d_c} in finite time. Here, without loss of generality, we assume that the goal q_{d_c} can be defined such as:

$$q_{d_c} = [\, 0 \;\; 0 \,]^\mathsf{T} \,. \tag{2-9}$$

Then, the control objective is simply described as:

$$q_c \rightarrow q_{d_c} \,, \qquad e_c = q_{d_c} - q_c \rightarrow 0 \,, \tag{2-10}$$

where $e_c \in \mathbb{R}^3$ is the Cartesian error given by:

$$e_c = \begin{bmatrix} e_x \\ e_y \end{bmatrix} = - \begin{bmatrix} x \\ y \end{bmatrix} . \tag{2-11}$$

Given the desired configuration q_{d_c} and the error e_c, it is possible propose a Theorem that ensures that the error goes to zero, as well the TMR reaches the desired configuration q_{d_c}.

Theorem 2.1 *(Cartesian Controller for Tracked Mobile Robots)*
Consider the kinematic model for the Tracked Mobile Robot (2-3) *and the assumptions mentioned in section 2.2.1. Assume the desired configuration* q_{d_c}

is norm-bounded. The following Cartesian control laws:

$$\begin{aligned} v &= k_1\left(e_x \cos\theta + e_y \sin\theta\right) \text{ and} \\ \omega &= k_2\left(e_x \sin\theta - e_y \cos\theta\right) , \end{aligned} \tag{2-12}$$

ensure the stabilization of the Cartesian error (e_x, e_y) *to zero, where* $k_1 > 0$ *and* $k_2 > 0$ *are control gains,* $v \in \mathbb{R}$ *is the linear velocity and* $\omega \in \mathbb{R}$ *is the angular velocity.*

In this theorem is verified that the Cartesian controller for a unicycle model defined in [2] can be applied to TMR. Additionally, Theorem 2.1 defines a Cartesian controller, that is able to control the two coordinates x and y, ensuring that the error in those coordinates will go to zero. This approach can be used when a TMR has to reach different goal point without regarding the orientation, in task such as monitoring, surveillance, surveying.

Proof. For proof, please see the Appendix A.1. ■ .

2.3.1.2 Verification

In this section, different tests will be presented to verify the performance of the Cartesian controller, the soil parameter k will be vary, then the controller gains k_1 and k_2, different initial positions will be used and finally the kinematic model will have some uncertainties.

Table 2.1: Initial configurations for TMR.

Initial Configuration	x**(m)**	y **(m)**	θ **(rad)**
C_1	1.5	1.5	$\frac{\pi}{2}$
C_2	-1.5	1.5	$\frac{\pi}{2}$
C_3	-1.5	-1.5	$\frac{\pi}{2}$
C_4	1.5	-1.5	$\frac{\pi}{2}$

As was previously explained, regulation task is driving the robot from any configuration q_c to $q_{d_c} = \begin{bmatrix} 0 & 0 \end{bmatrix}^{\mathsf{T}}$. Then, in order to verify the regulation task, the controller parameters are modified and show the behavior of the TMR, then the different initial configurations are used for the initial configuration of the robot as are shown in Table 2.1.

First Test Theorem 2.1 shows the control law for regulation of the Tracked Mobile Robot using Cartesian approach, this controller drives the

TMR to any configuration in the inertial frame, the kinematic model (2-3) has a factor to indicate the slippage d (2-8), in this test it will be studied the behavior of the controller in front of the variation of the value of k.

Table 2.2: Different configurations on slippage gain of the TMR

Configuration	k
C_1	0.01
C_2	0.1
C_3	0.5
C_4	1.0

In this simulation, the parameter k in equation (2-8) will vary according to the Table 2.2 and the robot will go from the same initial configuration $q_0 = \begin{bmatrix} 1.5 & 1.5 & \frac{\pi}{2} \end{bmatrix}^\mathsf{T}$.

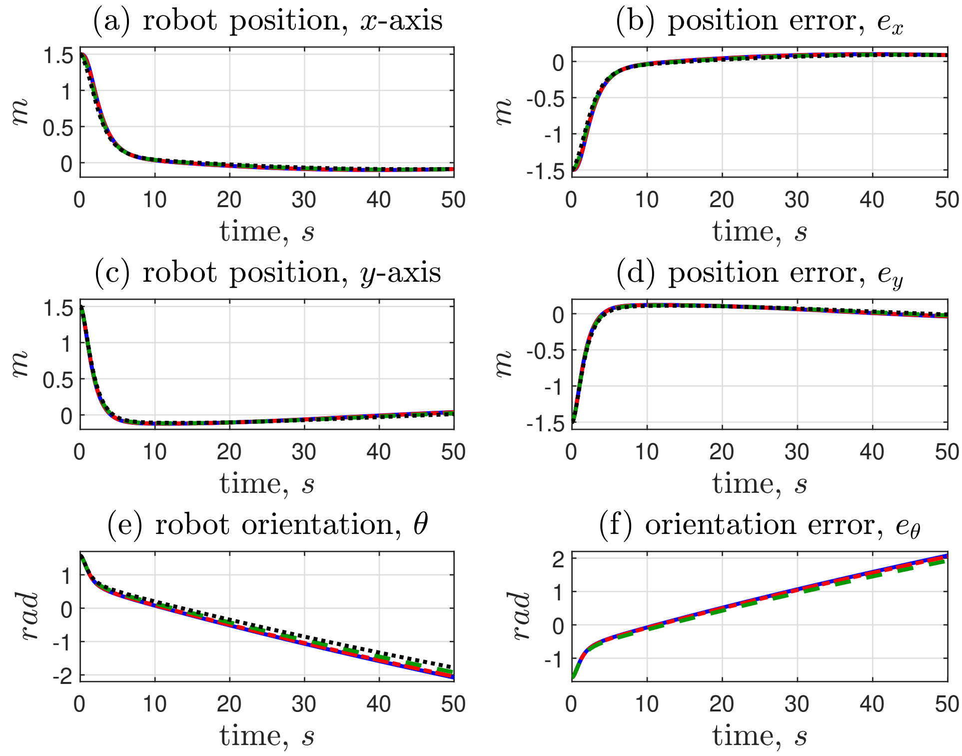

Figure 2.4: Simulation results: (a) robot position in the x-axis over time; (b) robot position in the y-axis over time. Legend: C1 (–), C2 (–.), C3 (– –), C4 (. .).

As a result of the simulation, in Figure 2.4 can be observed the position and error of the different coordinates of the TMR $q = [\,x\ y\ \theta\,]^\mathsf{T}$. It can be seen that there are no major changes in the results of the final robot position.

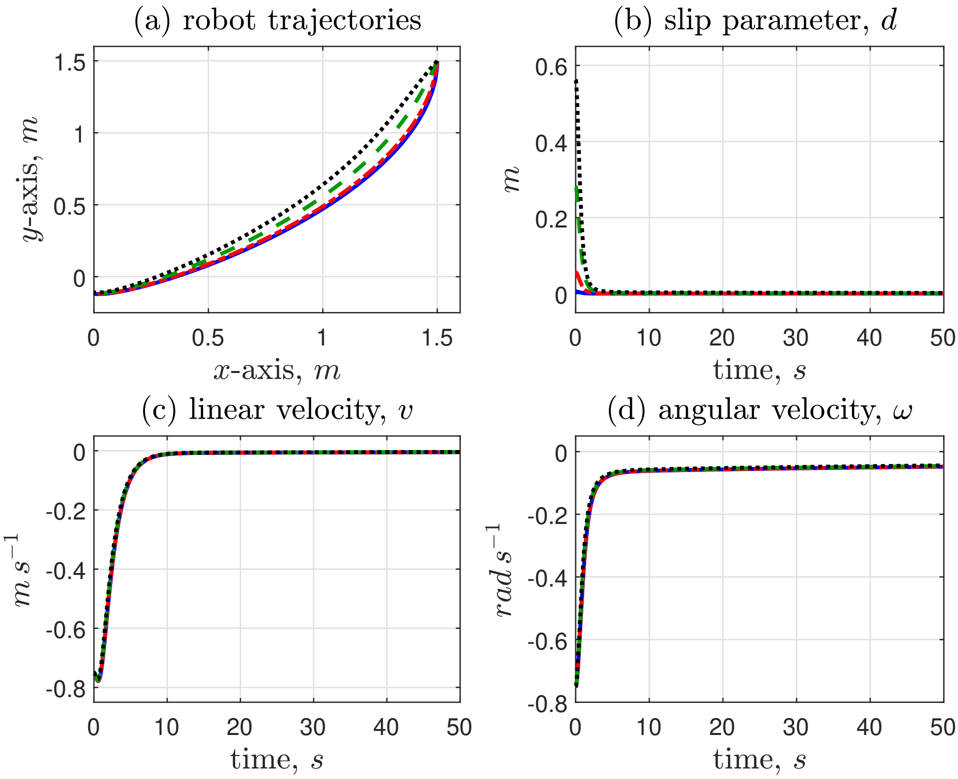

Figure 2.5: Simulation results: (a) robot trajectories in the xy plane; (b) robot orientation θ over time; (c) linear velocity v over time; (d) angular velocity ω over time. Legend: C1 (−), C2 (−.), C3 (− −), C4 (. .).

In Figure 2.5, it is observed that there are different results in the variation of the parameters: in the 2.5 (a) can be seen the trajectories generated for the robot, can be seen as the parameter k is bigger the cureve trajectory is more noticeable . The Figure 2.5 (b) shows the behavior of the slip parameter it can be seen the variation of the parameter k influence directly, in Figure 2.5 (c), (d) it is shown the control inputs, they converge to zero.

As a conclusion can be observed that the variation of the parameter k has influence in the trajectory and the slip parameter, having major resistance to reach the goal, describing a curve trajectory as the factor k is bigger. In the other figures can be seen that there is no major variation.

Second Test Theorem 2.1 shows the controller the Tracked Mobile Robot in Cartesian approach, it has two different control gains k_1 and k_2, that are going to be vary in the test.

Table 2.3: Different parameters on gain controllers of Cartesian Controller

Configuration	k_1	k_2
C_1	0.5	0.5
C_2	0.5	1.0
C_3	1.0	1.5
C_4	1.5	1.5

In this simulation, the parameters in the control law (2-12) k_1 and k_2 will vary according to the Table 2.3 and the robot will go from the same initial configuration $q_0 = \begin{bmatrix} 1.5 & 1.5 & \frac{\pi}{2} \end{bmatrix}^\mathsf{T}$.

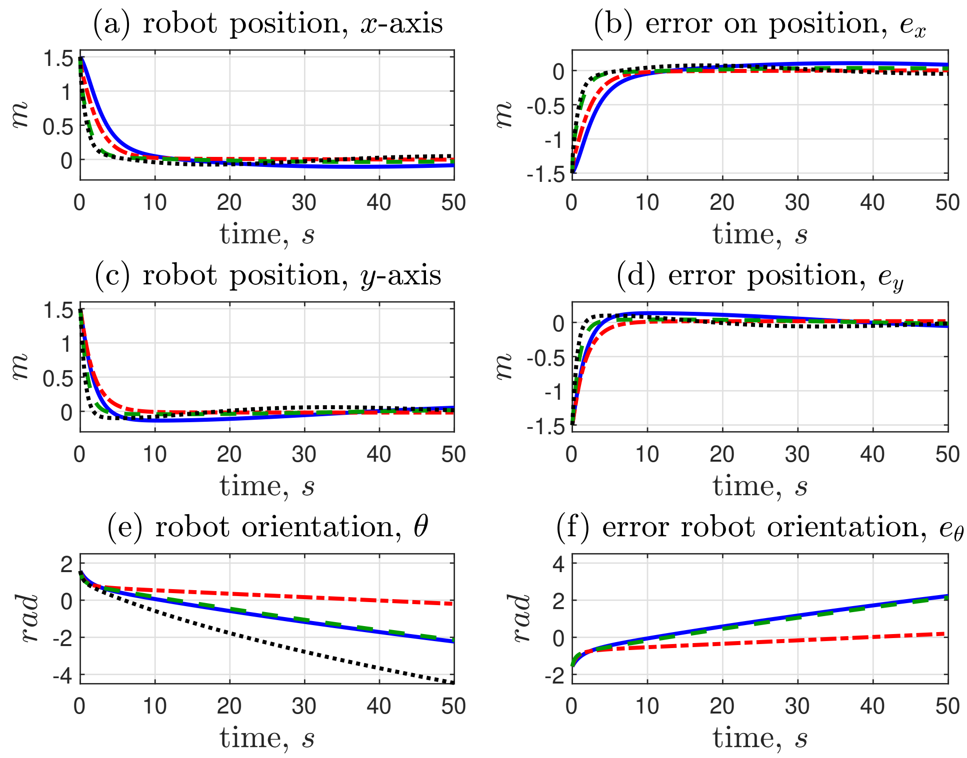

Figure 2.6: Simulation results: (a) robot position in the x-axis over time; (b) robot position in the y-axis over time. Legend: C1 (–), C2 (–.), C3 (– –), C4 (. .).

Figure 2.6, it can be observed the position and error of the different coordinates of the TMR $q = [x\ y\ \theta]^\mathsf{T}$. Notice that as minor the parameters are, the robot reaches the desired configuration taking more time. On the other hand, when the parameters of the controller are bigger, the robot coordinates will reach the desired configuration faster 2.6 (a) , (b) . It can be remark that the final orientation is not the objective of this controller.

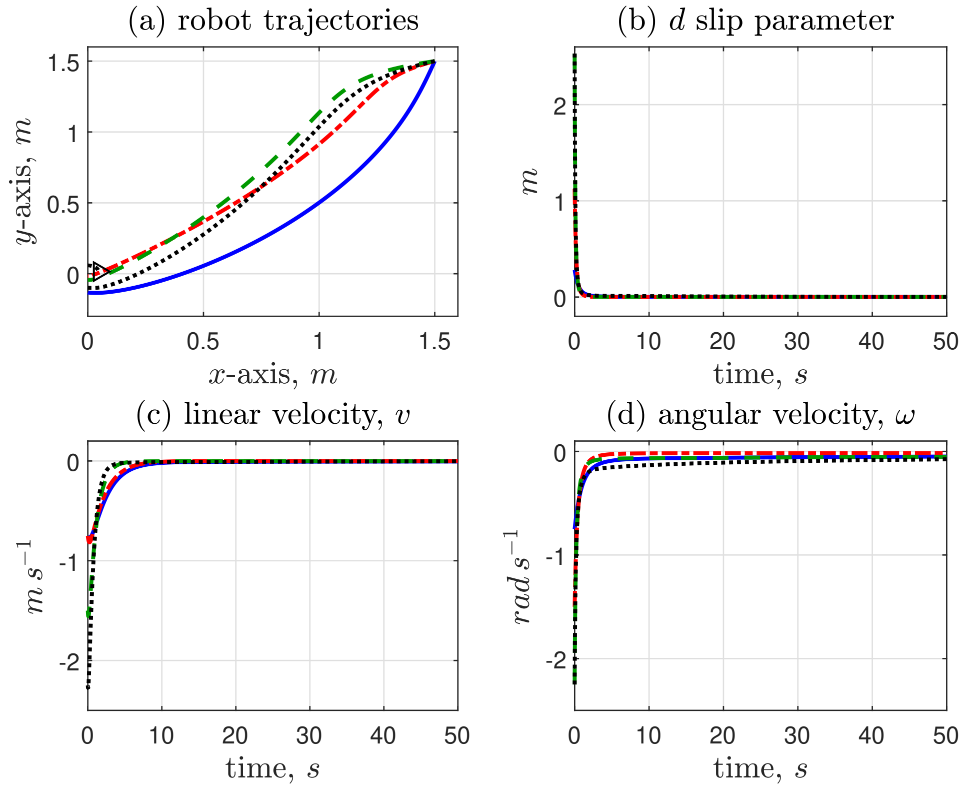

Figure 2.7: Simulation results: (a) robot trajectories in the xy plane; (b) robot orientation θ over time; (c) linear velocity v over time; (d) angular velocity ω over time. Legend: C1 (–), C2 (–.), C3 (– –), C4 (..).

In Figure 2.7, it is observed that there are different results in the variation of the parameters: in the 2.7 (a) can be seen the trajectories generated for the robot, the robot will reach the desired configuration but describing different trajectories. The Figure 2.7 (b) shows the behavior of the slip parameter it can be seen that there is no significant variation, in Figure 2.7 (c), (d) it is shown the control inputs, they converge to zero.

As a conclusion we can observe that increasing the parameters will cause that the trajectory be curved, but in the other parameters such as velocities and slip factor there is a no relevant variation.

Third Test In the third test, four different initial configurations of the Tracked Mobile Robot are considered, according the to the Table 2.1. The controller parameters used were $k_1 = 0.5$ and $k_2 = 0.5$

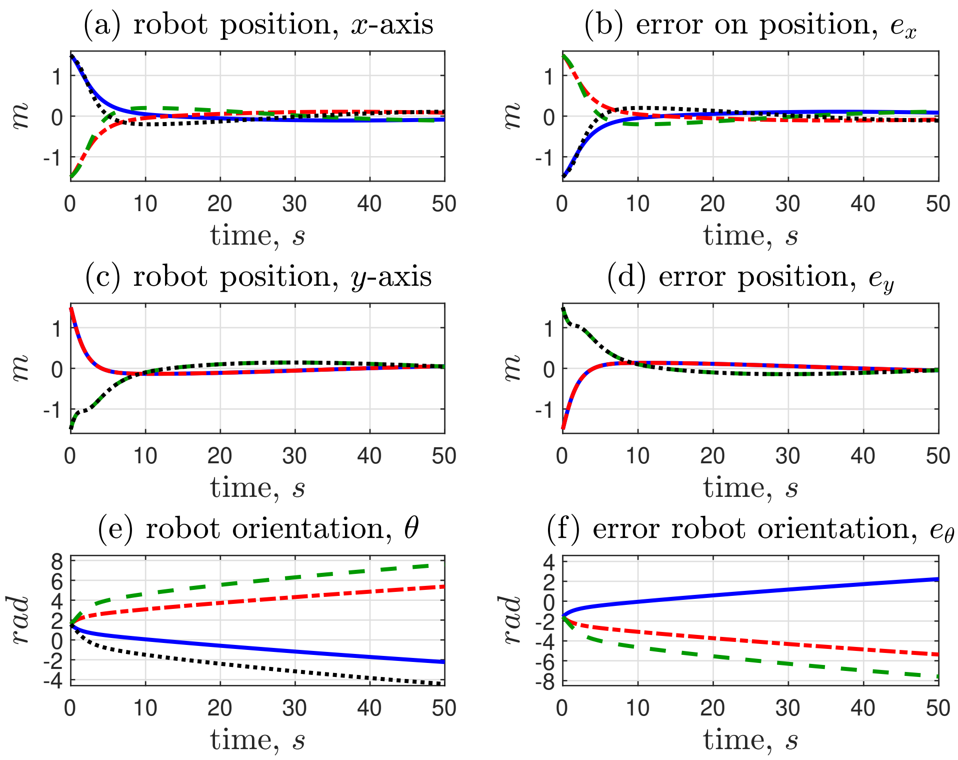

Figure 2.8: Simulation results: (a) robot position in the x-axis over time; (b) robot position in the y-axis over time. Legend: C1 ($-$), C2 ($-.$), C3 ($--$), C4 ($..$).

Figure 2.8 shows the behavior of the position and error of the different coordinates of the TMR $q = [\, x \ y \ \theta \,]^\mathsf{T}$, it can be observed that the coordinates reach the desired configuration and the error is close to zero.

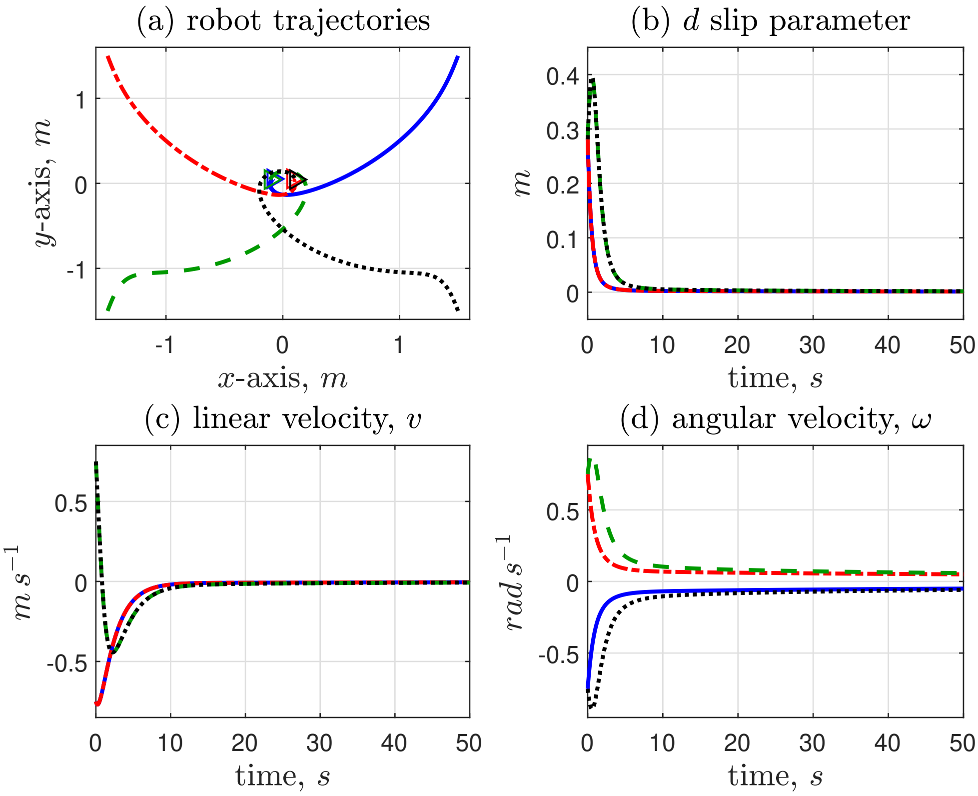

Figure 2.9: Simulation results: (a) robot trajectories in the xy plane; (b) robot orientation θ over time; (c) linear velocity v over time; (d) angular velocity ω over time. Legend: C1 (—), C2 (–.), C3 (– –), C4 (. .).

In Figure 2.9 (a) the robot trajectories can be observed: the robot reaches the desired configuration, although, at the end of the trajectory the configuration it follows a little circular trajectory. Figure 2.9 (b) shows the slip parameter as the robot describes a curved trajectory the slip parameter increments. In Figure 2.7(c) (d) is shown the control inputs, the linear velocity converges to zero as was mentioned in Theorem 2.1.

As a conclusion, can be observed that the robot reaches the desired configuration starting at any quadrant, additionally the coordinates x and y are reached, about the orientation can be said that the controller is not capable to control it.

2.3.2 Polar Coordinates based controller

This section describes a polar coordinates approach for the control design of Tracked Mobile Robot, as the formulation of a theorem that ensures the stabilization (regulation) of the TMR to the origin based on the existing approach [70] using the kinematic model described in equation (2-3).

A transformation to polar coordinates approach is applied in the kinematic model in equation (2-3), then a controller is proposed and, finally, a linearization is applied in order to obtain the stability analysis.

2.3.2.1 Control Design

As it was mentioned before, the regulation problem consists of going from a determined configuration q to a desired configuration q_d. Now defining the desired $q_d = [\, x_d \;\; y_d \;\; \theta_d \,]^\mathsf{T}$, the problem reduces to going from $q = [\, x \;\; y \;\; \theta \,]^\mathsf{T}$ to the goal.

Now, without loss of generality, the q_d is defined such as:

$$q_d = \begin{bmatrix} 0 \\ 0 \\ 0 \end{bmatrix} . \tag{2-13}$$

Then, Cartesian error is defined as :

$$e_p = q - q_d \ ,$$

$$e_p = - \begin{bmatrix} x \\ y \\ \theta \end{bmatrix} . \tag{2-14}$$

A transformation from Cartesian coordinates $q = [\, x \;\; y \;\; \theta \,]^\mathsf{T}$ to polar coordinates $p = [\, \rho \;\; \alpha \;\; \beta \,]^\mathsf{T}$ is given by [70]:

$$\begin{aligned} \rho &= \sqrt{x^2 + y^2} \,, \\ \alpha &= -\theta - atan2(y, x) \,, \\ \beta &= \theta - \alpha. \end{aligned} \tag{2-15}$$

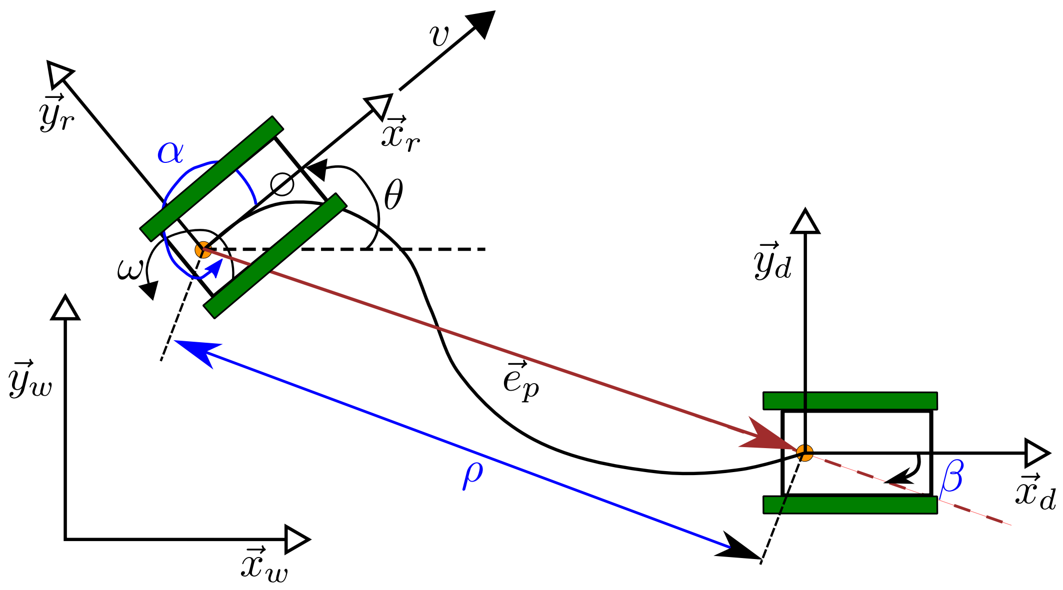

Figure 2.10: Polar Coordinates Definition.

These polar coordinates mentioned in equation (2-15), can be observed in the Figure 2.10, in which the inertial, robot $\mathcal{F}_r$ and desired frame $\mathcal{F}_d$ are showed. There are also the distance ρ is shown, and the angles α and β.

It is necessary to define a new Kinematic model based on the definitions of polar coordinates, it means find the vector of $\dot{p} = [\,\dot{\rho}\ \dot{\alpha}\ \dot{\beta}\,]^{\mathsf{T}}$. Firstly, we find $\dot{\rho}$ deriving with respect to time using the equation (2-15):

$$\dot{\rho} = \frac{1}{\rho}\,(x\dot{x} + y\dot{y}) \ \ .$$

Now, replacing the kinematic model described in the equation (2-3) in the above equation:

$$\begin{aligned}\dot{\rho} &= \frac{1}{\rho}\,(x\,(v\cos\theta + d\omega\sin\theta) + y\,(v\sin\theta - d\omega\cos\theta))\ \ , \\ &= \frac{1}{\rho}\,(v\,(x\cos\theta + y\sin\theta) + \omega d\,(x\sin\theta - y\cos\theta))\ \ .\end{aligned}$$

From the polar coordinates definition in (2-15) and Figure 2.10, it is known that $x = \rho\cos(\theta+\alpha)$ and $y = \rho\sin(\theta+\alpha)$, then:

$$\begin{aligned}\dot{\rho} = \ & \frac{v}{\rho}\,(\rho\cos(\theta+\alpha)\cos\theta + \rho\sin(\theta+\alpha)\sin\theta) + \\ & \frac{\omega d}{\rho}\,(\rho\cos(\theta+\alpha)\sin\theta - \rho\sin(\theta+\alpha)\cos\theta)\ \ ,\end{aligned}$$

finally $\dot{\rho}$ is:

$$\dot{\rho} = v\cos\alpha - d\omega\sin\alpha\,. \tag{2-16}$$

Now, finding $\dot{\alpha}$ using the kinematic model in equation (2-3) and the polar coordinates definition (2-15):

$$\begin{aligned}
\dot{\alpha} &= -\omega + \frac{\frac{d}{dt}\left(\frac{y}{x}\right)}{1+\left(\frac{y}{x}\right)^2} \\
&= -\omega + \frac{\frac{\dot{y}x - y\dot{x}}{x^2}}{\frac{x^2+y^2}{x^2}} \\
&= -\omega + \frac{\dot{y}x - y\dot{x}}{\rho^2} \\
&= -\omega + \frac{x\left(v\sin\theta - d\omega\cos\theta\right) - y\left(v\cos\theta + d\omega\sin\theta\right)}{\rho^2} \\
&= -\omega + \frac{\rho\cos(\theta+\alpha)\left(v\sin\theta - d\omega\cos\theta\right) - \rho\sin(\theta+\alpha)\left(v\cos\theta + d\omega\sin\theta\right)}{\rho^2} \\
&= -\omega + \frac{v}{\rho}\left[\cos(\theta+\alpha)\sin\theta - \sin(\theta+\alpha)\cos\theta\right] - \\
&\quad \frac{\omega d}{\rho}\left[\cos(\theta+\alpha)\cos\theta + \sin(\theta+\alpha)\sin\theta\right]
\end{aligned},$$

Finally $\dot{\alpha}$ is:

$$\dot{\alpha} = -\omega - \frac{v\sin\alpha}{\rho} - \frac{d\omega\cos\alpha}{\rho}\ . \tag{2-17}$$

In order to complete the new kinematic model it is necessary to compute $\dot{\beta}$:

$$\begin{aligned}
\dot{\beta} &= -\dot{\theta} - \dot{\alpha} \\
&= -\omega + \omega + \frac{v\sin\alpha}{\rho} + \frac{d\omega\cos\alpha}{\rho}\ ,
\end{aligned}$$

And, finally $\dot{\beta}$ is found:

$$\dot{\beta} = \frac{v\sin\alpha}{\rho} + \frac{d\omega\cos\alpha}{\rho}\ , \tag{2-18}$$

Now, joining the equations (2-16), (2-17) and (2-18):

$$
\begin{bmatrix} \dot{\rho} \\ \dot{\alpha} \\ \dot{\beta} \end{bmatrix} = \begin{bmatrix} \cos\alpha & -d\sin\alpha \\ \\ -\frac{1}{\rho}\sin\alpha & -1-\frac{d}{\omega}\cos\alpha \\ \\ \frac{1}{\rho}\sin\alpha & \frac{d}{\rho}\cos\alpha \end{bmatrix} \begin{bmatrix} v \\ \omega \end{bmatrix}, \tag{2-19}
$$

The equation (2-19) represents the Kinematic Model based on Polar coordinates. This new system is the objective of the controller to be designed in this section.

Theorem 2.2 *(Controller based on Polar Coordinates)*
Considering the kinematic modeling for the Tracked Mobile Robot (2-3)*, the coordinates transformation* (2-15) *and only small values for* α*. Assume the desired configuration* $q_d \in \mathbb{R}^3$ *is norm-bounded. The following control laws:*

$$
\begin{aligned} v &= k_\rho \rho \, and \\ \omega &= k_\alpha \alpha + k_\beta \beta \, , \end{aligned} \tag{2-20}
$$

ensure the stabilization of the posture error e_q *in equation* (2-14) *to zero, where* $v \in \mathbb{R}$ *is the linear velocity and* $\omega \in \mathbb{R}$ *is the angular velocity,* k_ρ*,* k_α*,* k_β *are the control gains that follow the next conditions in order to guarantee the stability:* $k_\rho > 0$ *,* $k_\beta < 0$ *and* $k_\alpha - k_\rho > 0$ *.*

These two control laws presented in the Theorem 2.2 are able to stabilize the system in equation (2-19) to the origin from any point, regarding the final orientation.
Proof. For proof, please see the Appendix A.2. ■

2.3.2.2 Verification

This section will present the numerical simulations for the polar coordinates controller. Four types of tests were performed as the previous controller. In the first test, the soil parameter is vary, the second test perform a variation on the gain controllers. The third test is performed varying the initial configurations according to the Table 2.1 and finally the fourth test increments to the kinematic model radio uncertainties.

First Test In the first test, the soil parameter k is varied according to the Table 2.2, in order to verify the behavior of the Polar Coordinate in front of different types of terrains.

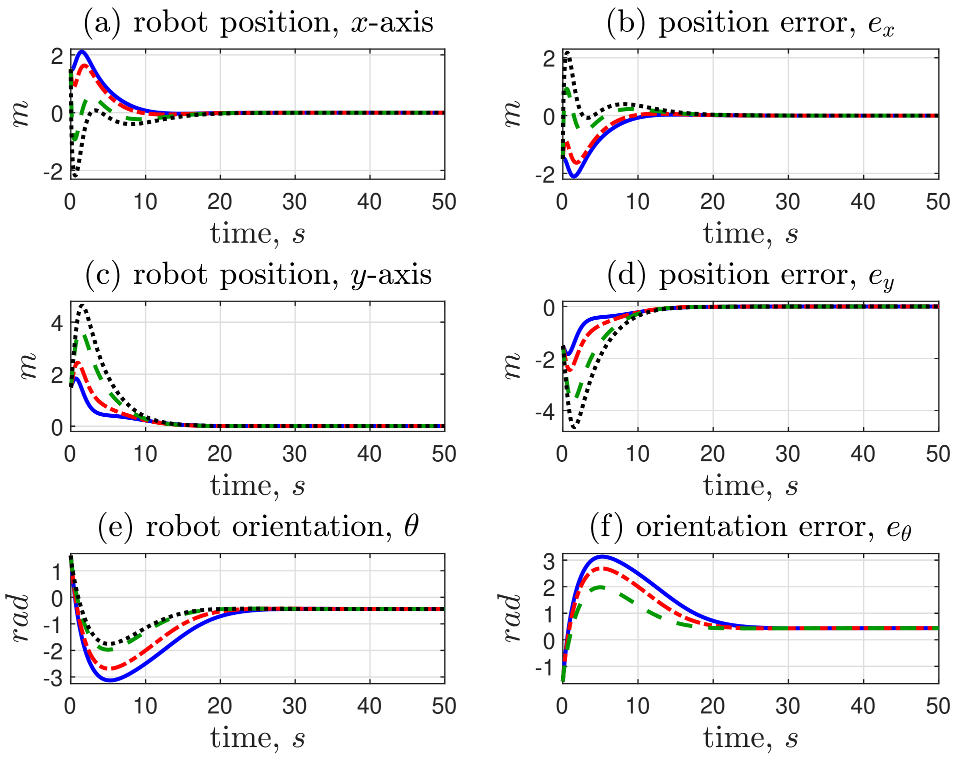

Figure 2.11: Simulation results: (a), (b) robot position and error in the x-axis over time; (c) (d) robot position and error in the y-axis over time; (e) (f) robot position and error in the θ-axis over time. Legend: C1 (−), C2 (−.), C3 (− −), C4 (. .).

In Figure 2.11, the results for the numerical simulations varying the gain of the terrain are shown. The different coordinates of the robot in real world $q = [\,x\ y\ \theta\,]^\mathsf{T}$ and its respective error. It can be observed that as smaller is the parameter k the robot has less movement in the axis y and y which should be a factor of the slippage, it means that if the robot is moving more it has more slippage because of the factor k. Can be shown that all the coordinates go to zero, including the errors.

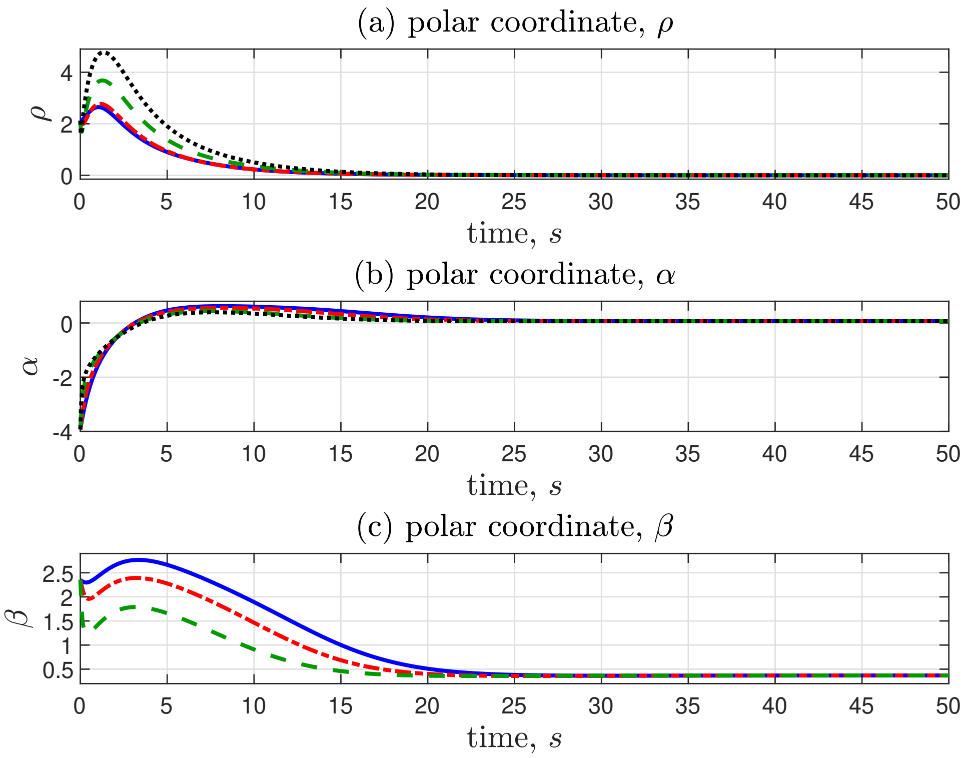

Figure 2.12: Simulation results: (a) polar coordinate ρ ; (b) polar coordinate α ; (b) polar coordinate β Legend: C1 ($-$), C2 ($-.$), C3 ($--$), C4 ($..$).

In Figure 2.12, the polar coordinates during the time are shown.It can be observed that all the coordinates are going to zero. The ρ coordinate shows the robot has more displacement in the axis x and y. In addition can be shown that the coordinates α and β, coordinates related to the orientation, take more time to converge.

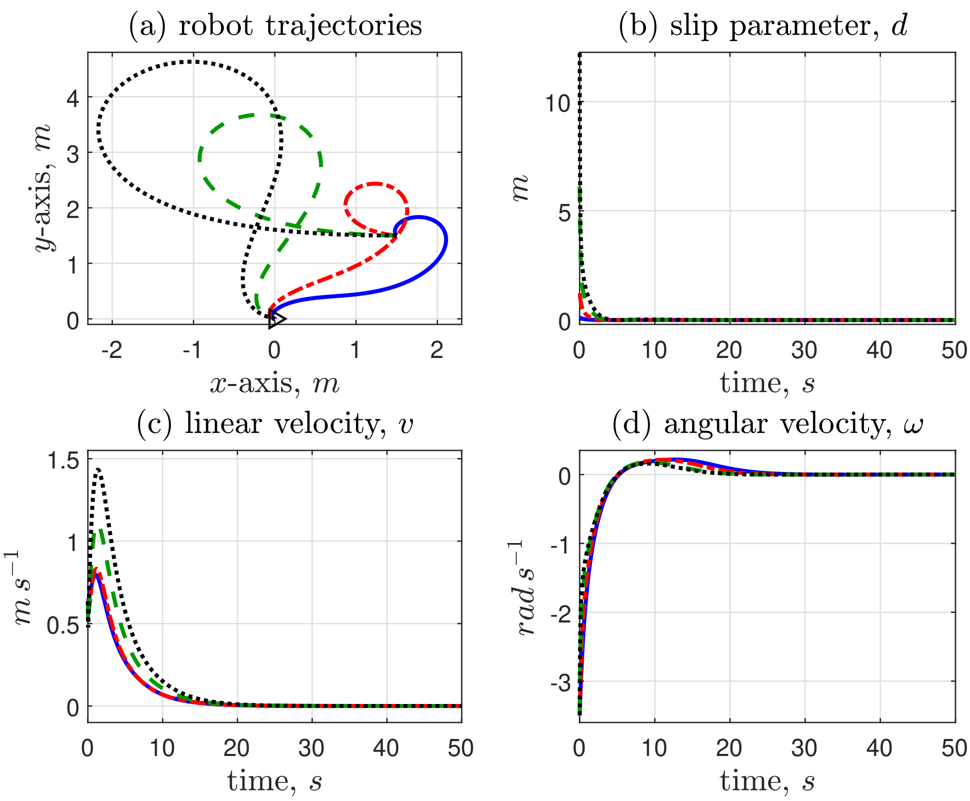

Figure 2.13: Simulation results: (a) robot trajectories in the xy plane; (b) parameter of slip d over time; (c) linear velocity v over time; (d) angular velocity ω over time. Legend: C1 (−), C2 (−.), C3 (− −), C4 (..).

Finally, in Figure 2.13 (a) is shown the different trajectories for the same goal and the same initial configuration, it can be noted that as the parameter k describes a more curved trajectory because of the slippage, Figure 2.13 (b) shows the slipping parameter which has more value as the parameter k is greater. In Figure 2.13 (c)(d) the linear v and angular velocity are shown, as can be note the parameter k are greater they control input are bigger.

Table 2.4: Different configurations of gains of Polar Coordinates Controller

Configuration	k_ρ	k_α	k_β
C_1	0.150	0.400	-0.075
C_2	0.300	0.800	-0.150
C_3	0.450	1.200	-0.225
C_4	0.600	1.600	-0.300

Second Test In the second test, the parameters in the controller are varied following the Table 2.4, these parameters will influence in the behavior of the robot.

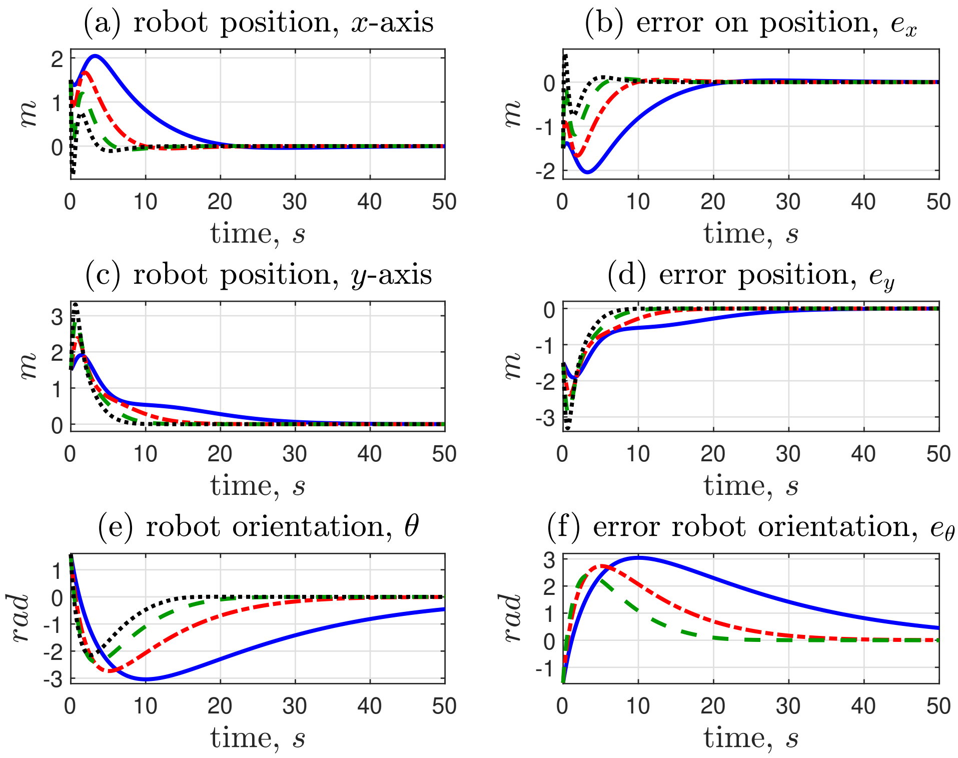

Figure 2.14: Simulation results: (a), (b) robot position and error in the x-axis over time; (c) (d) robot position and error in the y-axis over time; (e) (f) robot position and error in the θ-axis over time. Legend: C1 (—), C2 (–.), C3 (– –), C4 (. .).

In Figure 2.14, the results for the numerical simulations varying the gain controllers are shown, the different coordinates of the robot in real world $q = [x\ y\ \theta]^\mathsf{T}$ and its respective error. It can be observed that minor are the parameters the robot takes more time to reach the origin desired value.

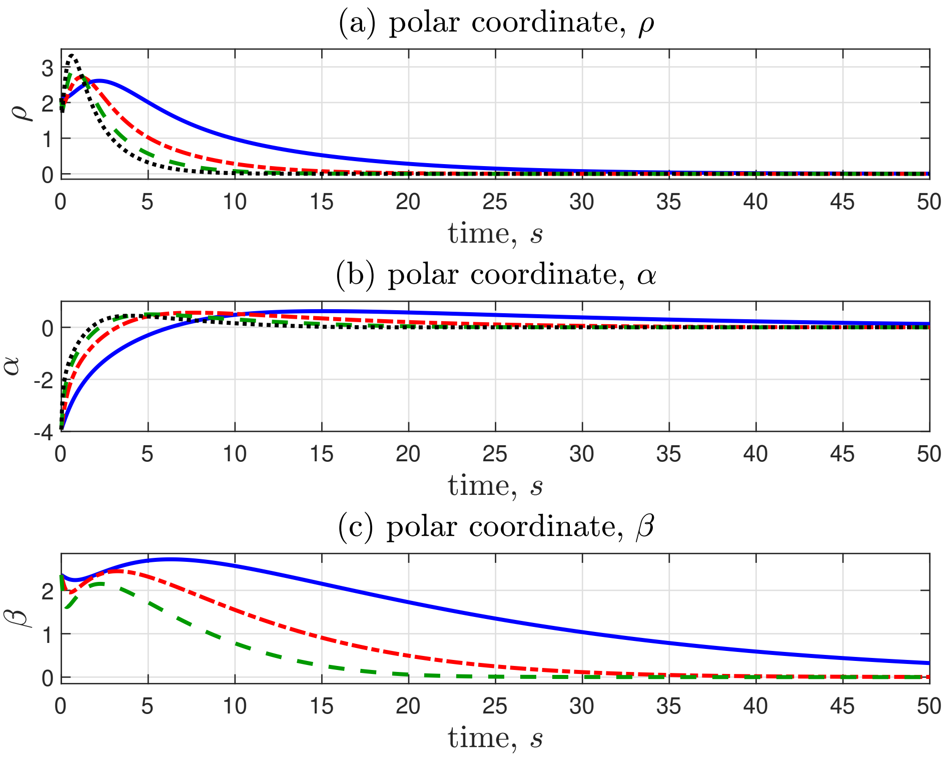

Figure 2.15: Simulation results: (a) polar coordinate ρ ; (b) polar coordinate α ; (b) polar coordinate β Legend: C1 ($-$), C2 ($-.$), C3 ($--$), C4 ($..$).

In Figure 2.15, the polar coordinates during the time are shown. β coordinate takes more time to converge than the other polar coordinates, as effect of the increasing the controller gains.

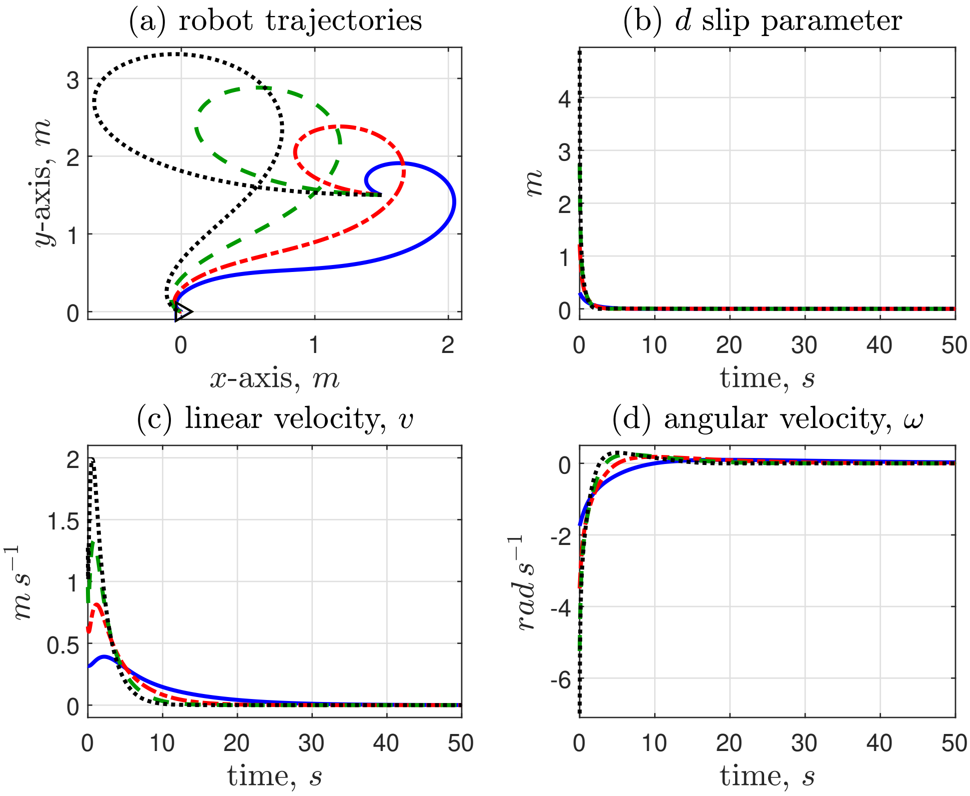

Figure 2.16: Simulation results: (a) robot trajectories in the xy plane; (b) parameter of slip d over time; (c) linear velocity v over time; (d) angular velocity ω over time. Legend: C1 (−), C2 (−.), C3 (− −), C4 (. .).

Finally, in Figure 2.16 (a) is shown the different trajectories for the same goal and the same initial configuration, it can be noted that as the parameters are greater the robot describes a more curved trajectory, Figure 2.16 (b) shows the slipping parameter which has not mayor variation. In Figure 2.16 (c)(d) the linear and angular velocity is shown, as can be note the parameter are greater they control input are bigger.

Third Test The third test, as were made in the Cartesian controller, is about varying the initial configuration for the robot, according to the Table 2.1.

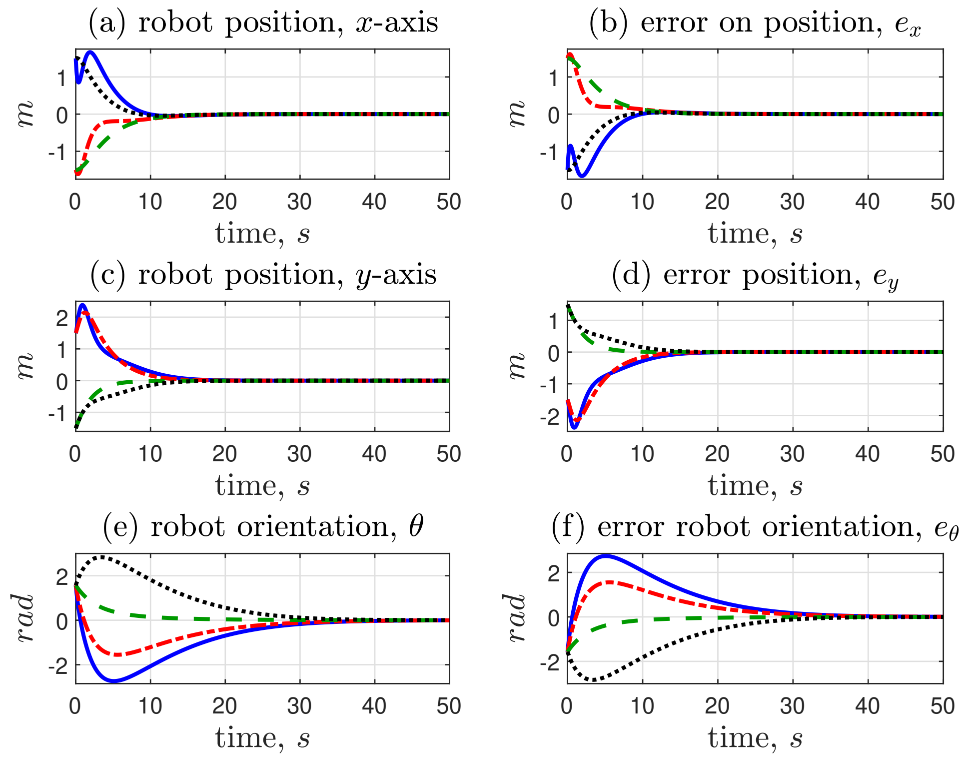

Figure 2.17: Simulation results: (a), (b) robot position and error in the x-axis over time; (c) (d) robot position and error in the y-axis over time; (e) (f) robot position and error in the θ-axis over time. Legend: C1 (−), C2 (−.), C3 (− −), C4 (..).

In Figure 2.17, the variation in the coordinates and its errors are shown. It can be observed that the convergence to zero has similar rates for every initial configuration in the different quadrants.

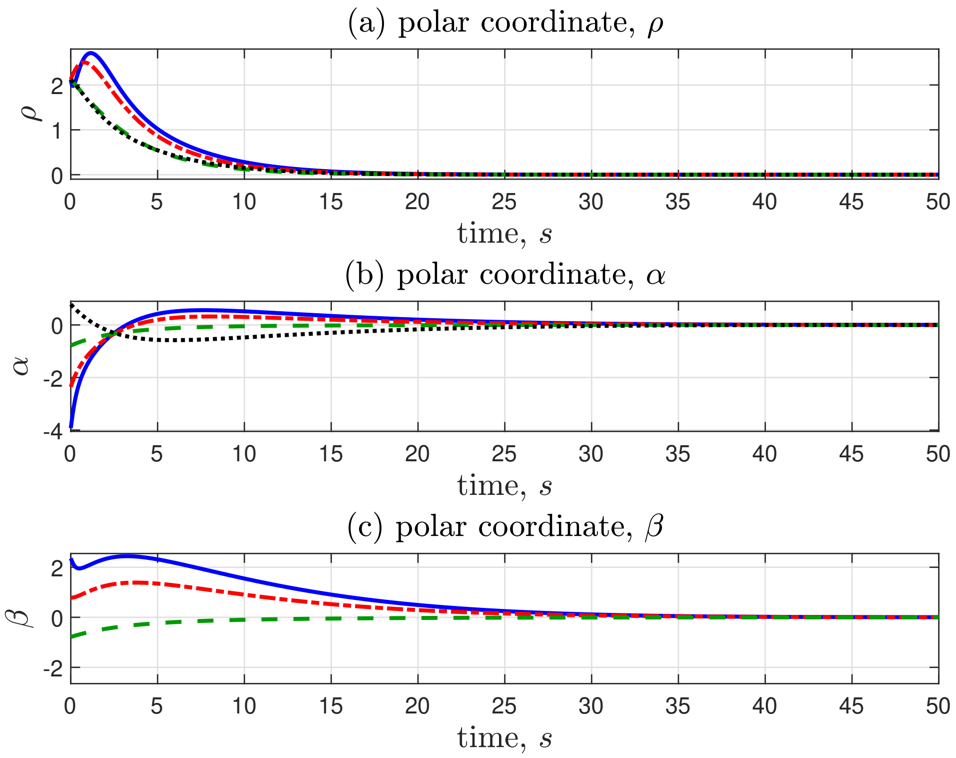

Figure 2.18: Simulation results: (a) polar coordinate ρ ; (b) polar coordinate α ; (b) polar coordinate β Legend: C1 (−), C2 (−.), C3 (− −), C4 (..).

Now, in Figure 2.18, the behavior of the polar coordinates are shown. It can be observed that the polar coordinate for the distance ρ is the fastest to converge.

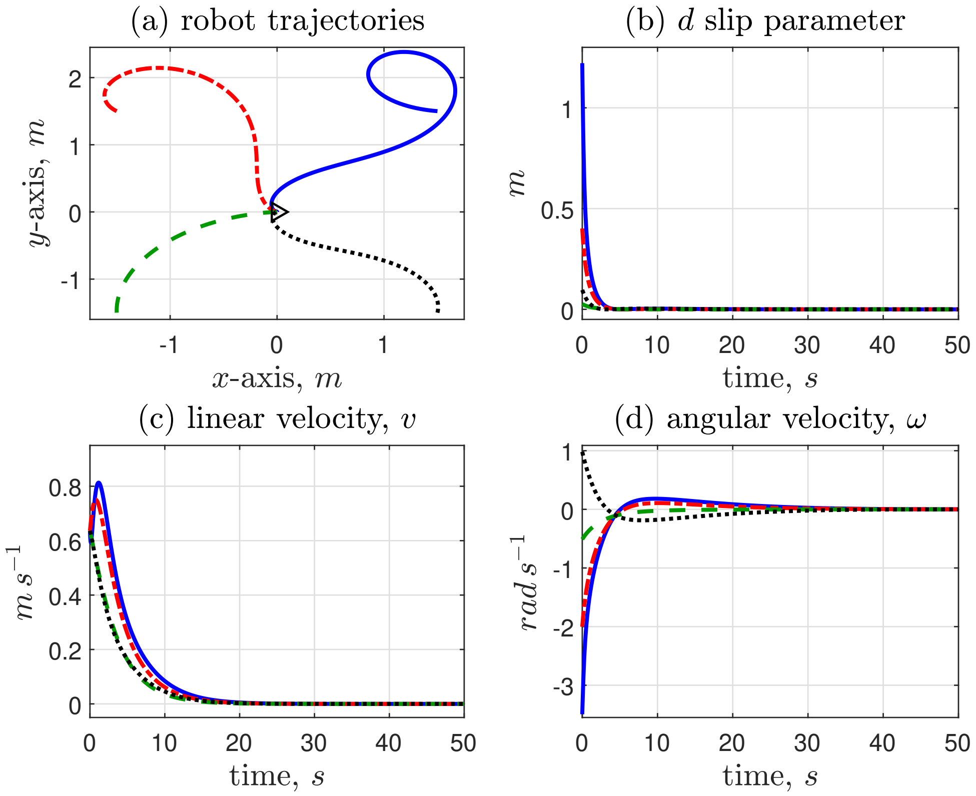

Figure 2.19: Simulation results: (a) robot trajectories in the xy plane; (b) parameter of slip d over time; (c) linear velocity v over time; (d) angular velocity ω over time. Legend: C1 (−), C2 (−.), C3 (− −), C4 (..).

Figure 2.19 (a) shows the different trajectories described by the robot in all the initial configurations the TMR reaches the desired configuration at the origin. Figure 2.19 (b) is the slipping parameter converging to zero, it can be observed that the robot has more curved trajectory the slipping parameter is greater because it depends of the angular velocity. Finally, Figure 2.19 (c) (d) shows the linear and angular velocity, it can be seen that the velocities converge to zero.

Fourth Test In the fourth test, uncertainties in the radio are increased, varying the equation (2-5) as follows:

$$\begin{bmatrix} \dot{\phi}_L \\ \dot{\phi}_R \end{bmatrix} = \frac{1}{r^* b^2} \begin{bmatrix} 1 & -\dfrac{b}{2} \\ 1 & \dfrac{b}{2} \end{bmatrix} \begin{bmatrix} v \\ \omega \end{bmatrix}, \tag{2-21}$$

where r^* is the uncertain radio.

This test also working varying the initial configuration for the robot, according to the Table 2.1.

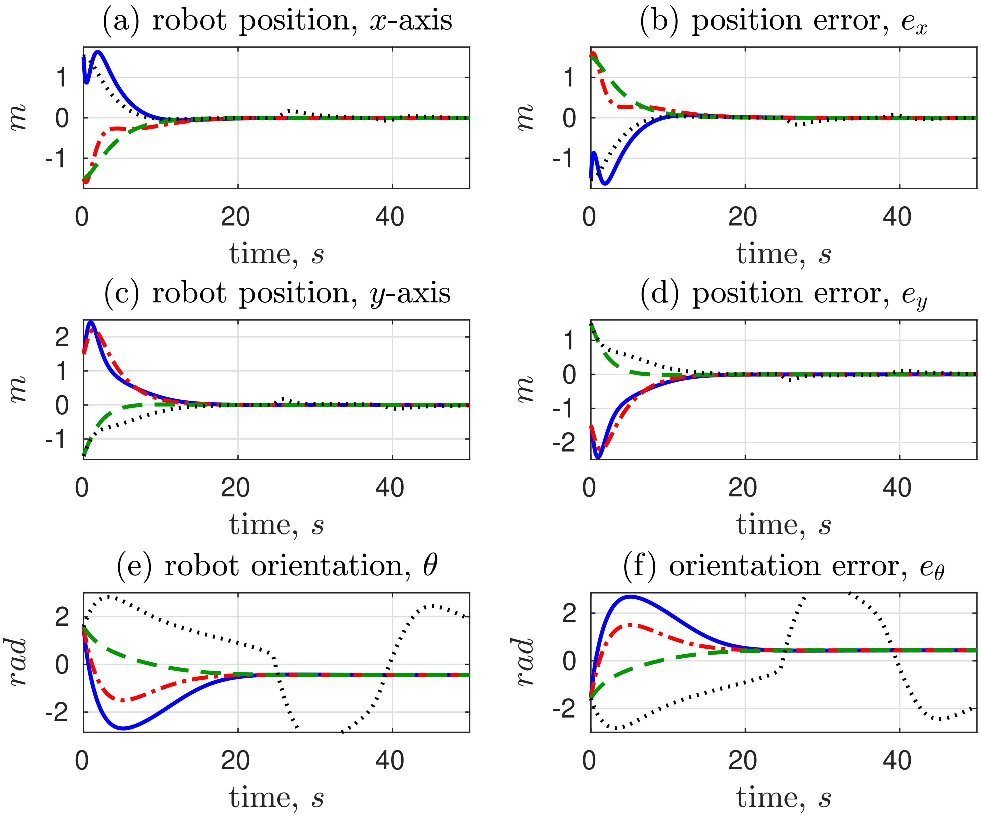

Figure 2.20: Simulation results: (a), (b) robot position and error in the x-axis over time; (c) (d) robot position and error in the y-axis over time; (e) (f) robot position and error in the θ-axis over time. Legend: C1 (−), C2 (−.), C3 (− −), C4 (. .).

In Figure 2.20, the variation in the coordinates and its errors are shown. It can be observed that in the configuration C_4 are troubles to reach the desired position because of the radio uncertainty.

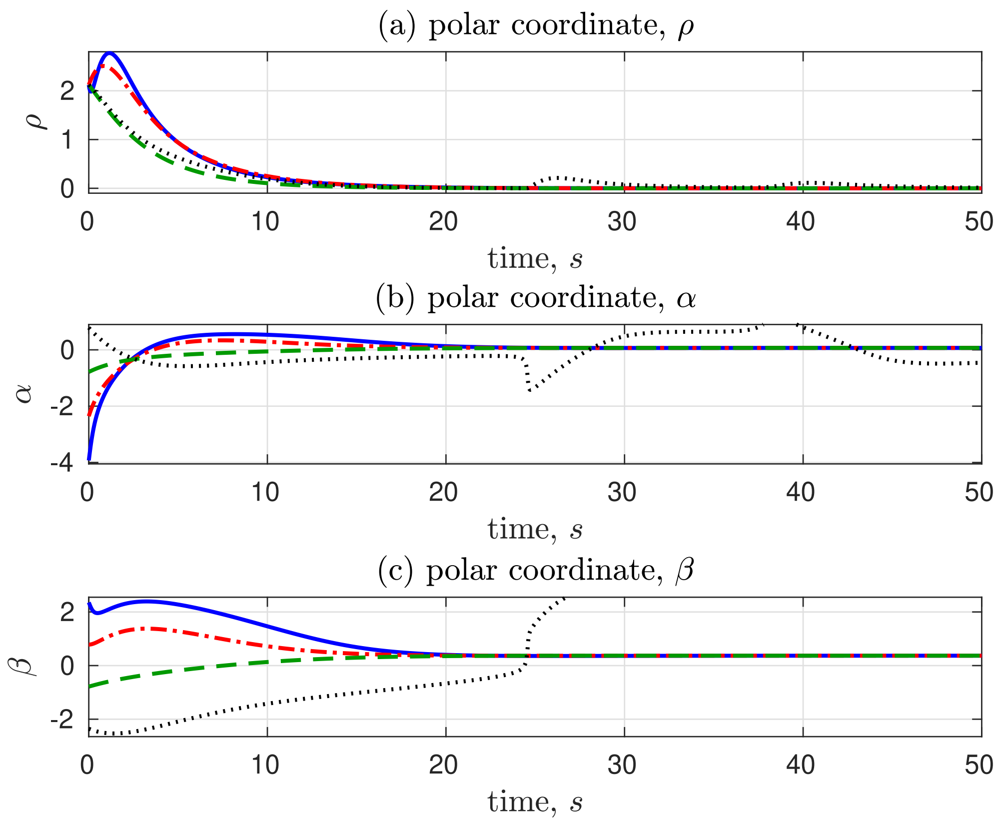

Figure 2.21: Simulation results: (a) polar coordinate ρ ; (b) polar coordinate α ; (b) polar coordinate β Legend: C1 (−), C2 (−.), C3 (− −), C4 (..).

Now, in Figure 2.21, the behavior of the polar coordinates are shown, it can be seen that all the polar coordinates have troubles to reach zero, mainly the α and β coordinates the unstable.

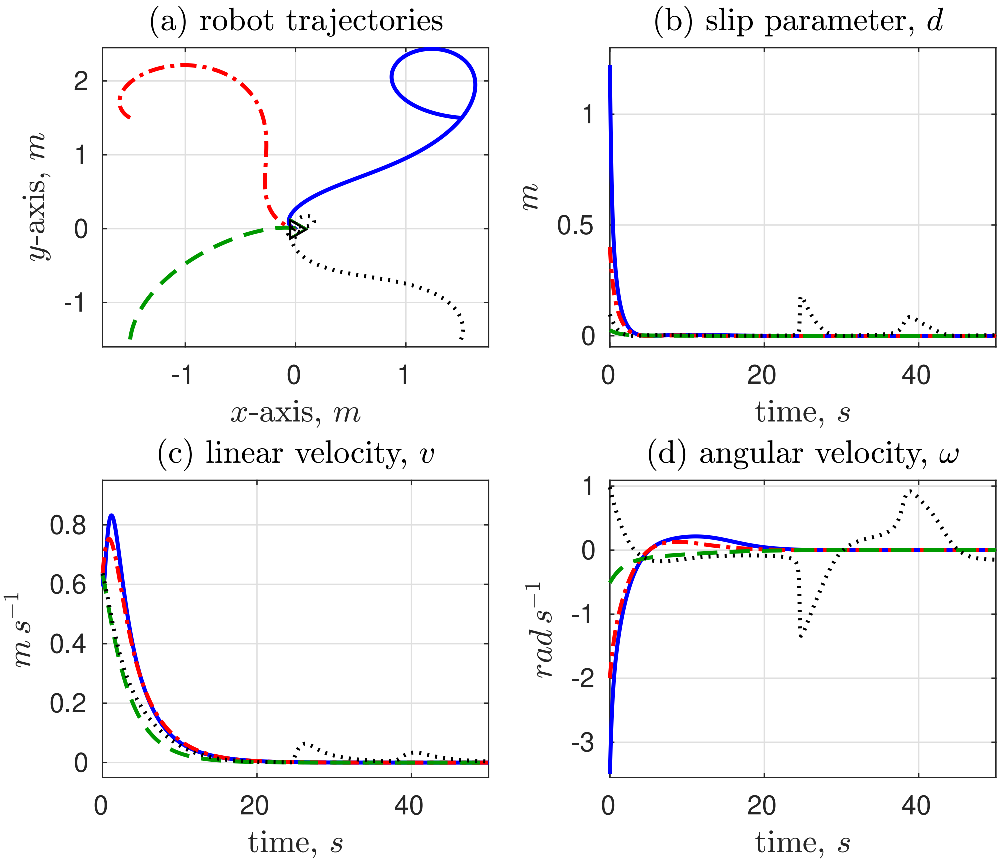

Figure 2.22: Simulation results: (a) robot trajectories in the xy plane; (b) parameter of slip d over time; (c) linear velocity v over time; (d) angular velocity ω over time. Legend: C1 (—), C2 (–.), C3 (– –), C4 (..).

Figure 2.22 (a) shows the different trajectories described by the robot in all the initial configurations, it has some problems to reach the desired configuration in C_4. Figure 2.22 (b) is the slipping parameter, can be observed that the configuration C_4 has troubles to stabilize the d factor. Finally, Figure 2.22 (c) (d) shows the linear and angular velocity, it can be observed the problems to stabilize in configuration C_4.

As a conclusion it can be mentioned that the controller can stabilize to the origin ensuring the convergence for all the coordinates, including the orientation, but when some disturbance are included the controller can not ensure the stabilization.